

In-sensor dynamic computing for intelligent machine vision

In the format provided by the
authors and unedited

Table of contents

Supplementary Fig. 1.

Schematic illustration of fabrication procedure for the graphene/Ge heterostructure device.

Supplementary Fig. 2.

Raman spectroscopy of Ge on the top of GeOI substrate and transferred graphene on SiO₂.

Supplementary Fig. 3.

Optoelectronic characteristics of the graphene/Ge heterostructure under light illumination of near-infrared 1550 nm.

Supplementary Fig. 4.

Photoresponse time for the graphene/Ge heterostructure under light illumination of 640 nm.

Supplementary Fig. 5.

Photoresponse characteristic of the graphene/Ge heterostructure with metal (Ti 3 nm/Au 25 nm) as top gate and 30 nm Al₂O₃ as gate dielectric material.

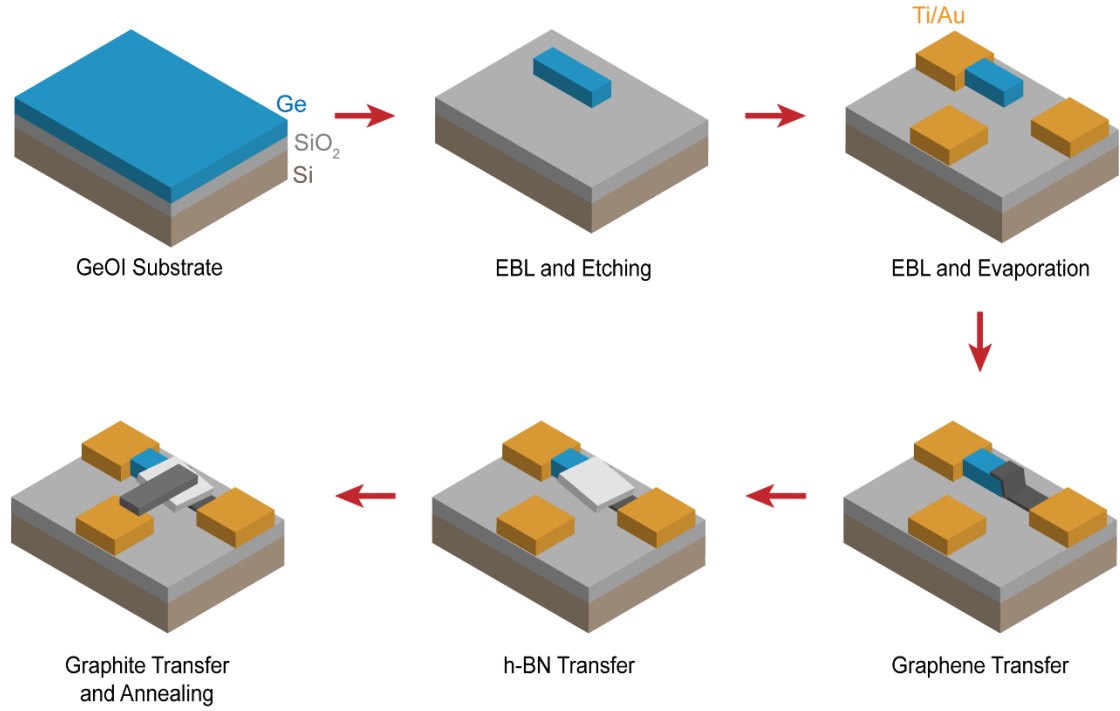
Supplementary Fig. 6.

Simulation results for the infrared image.

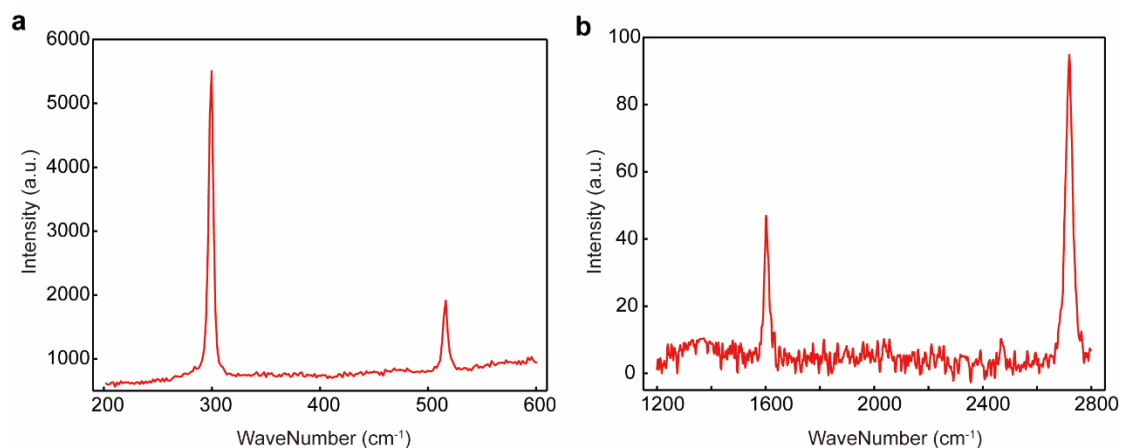
Supplementary Fig. 7.

Photograph of the experimental setups.

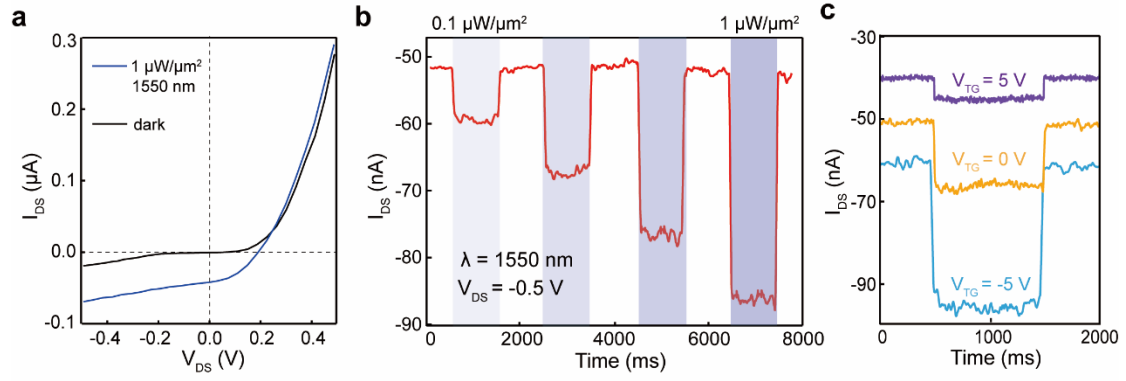
References.



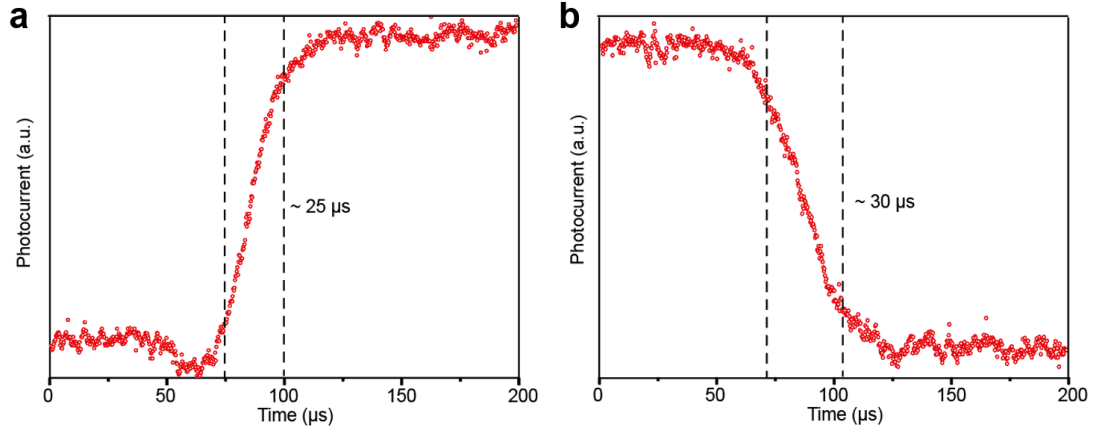
Supplementary Fig. 1. Schematic illustration of fabrication procedure for the graphene/Ge heterostructure device. The process started with germanium on insulator (GeOI) substrate. The source and drain metal contact of the device is Ti 5 nm/Au 30 nm. The thin film Ge exhibits a narrow bandgap and broadband light absorption from visible to infrared. The generated electron-hole pairs in the Ge under light excitation can be separated by strong built-in electrical field within the Schottky junction of graphene/Ge. The disassociated photo-generated carriers can be efficiently collected by using the graphene with ultrahigh carrier mobility [1,2]. Furthermore, the resulting photovoltaic response characteristics of mixed-dimensional heterostructure can be tailored via top and bottom gates to generate correlated behaviors in adjacent devices.



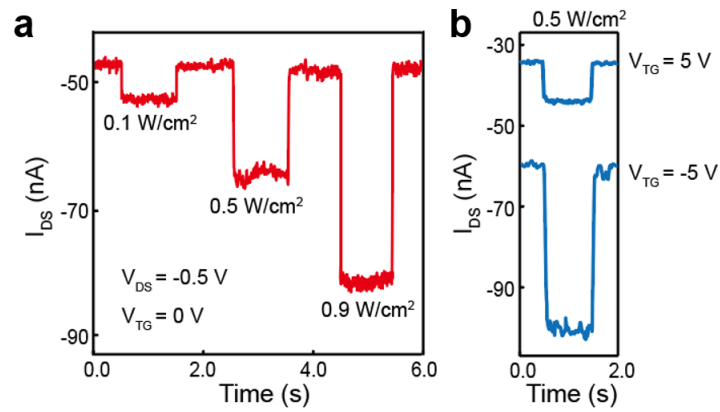
Supplementary Fig. 2. Raman spectroscopy of Ge on the top of GeOI substrate (a) and transferred graphene on SiO₂ (b). The Raman characteristic peak of Ge is situated at 300 cm⁻¹ while the Raman spectrum of bottom Si peaks at ~520 cm⁻¹. The Raman peaks of graphene include G peak (~1580 cm⁻¹) and 2D peak (~2700 cm⁻¹). The intensity ratio of the 2D peak to G peak is higher than 1, suggesting that graphene is in monolayer form. Besides, the D peak at ~1300 cm⁻¹ is not observed, indicating the graphene used in the experiment exhibits a perfect crystal lattice with few defects.



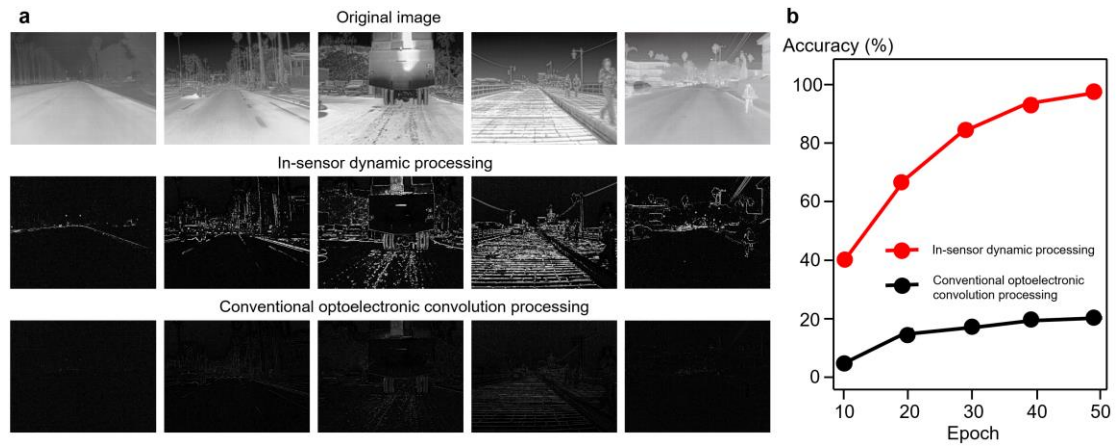
Supplementary Fig. 3. Optoelectronic characteristics of the graphene/Ge heterostructure under light illumination of near-infrared 1550 nm. a, I_{DS} - V_{DS} characteristics of the device with and without light illumination. **b,** Photoresponse of the device under 1550 nm light illumination of intensities from $0.1 \mu\text{W}/\mu\text{m}^2$, $0.4 \mu\text{W}/\mu\text{m}^2$, $0.7 \mu\text{W}/\mu\text{m}^2$ to $1 \mu\text{W}/\mu\text{m}^2$. **c,** Photoresponse measured at different V_{TG} under 1550 nm light illumination of $0.1 \mu\text{W}/\mu\text{m}^2$. Note that $V_{DS} = -0.5 \text{ V}$ and $V_{BG} = 0 \text{ V}$ for the experimental measurement.



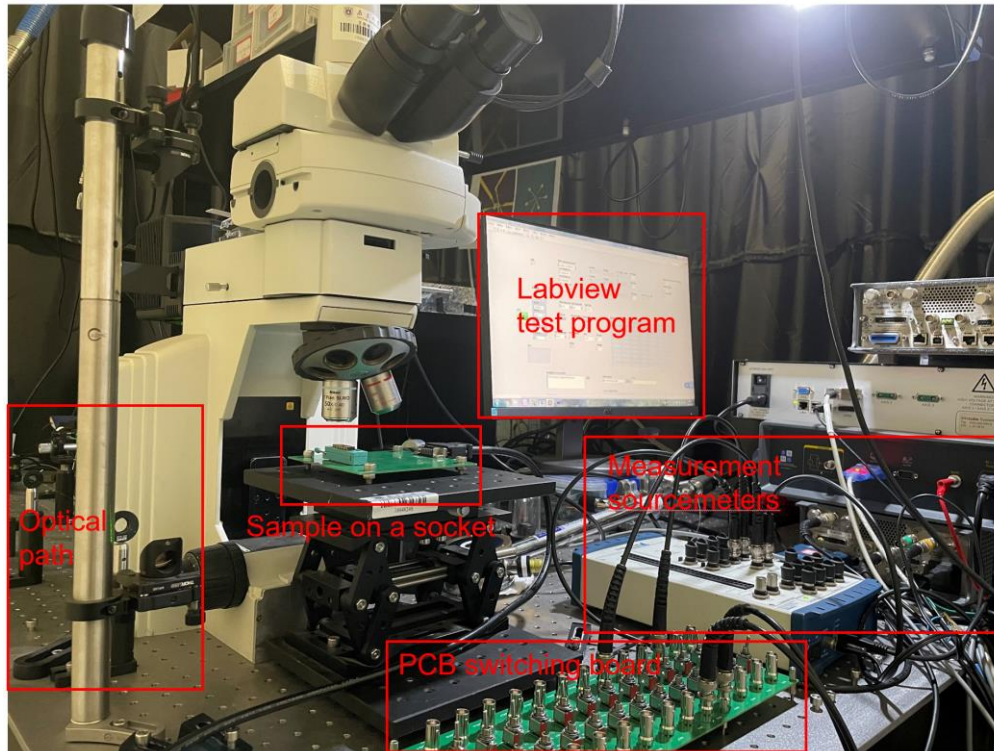
Supplementary Fig. 4. Photoresponse time for the graphene/Ge heterostructure under light illumination of 640 nm. The rise time (a) and fall time (b) is about 25 μs and 30 μs, respectively.



Supplementary Fig. 5. Photoresponse characteristic of the graphene/Ge heterostructure with metal (Ti 3 nm/Au 25 nm) as top gate and 30 nm Al₂O₃ as gate dielectric material. a, Photoresponse of the device under 640 nm light illumination of different intensities. b, Photoresponse of the device under different top gate voltage at a fixed light intensity.



Supplementary Fig. 6. Simulation results for the infrared image. **a**, Original images and its corresponding edge feature extraction results based on our in-sensor dynamic correlated processing and conventional convolutional processing. **b**, Recognition accuracy of five scenarios by our pixel-correlated computing technology and traditional convolution processing followed by the same ANN. The five scenarios include empty street, cars on street, train on street, pedestrian on street and cyclist on street. All the images exhibit same greyscale range from 0 to 255. The infrared images were adopted from FLIR_ADAS dataset, which is an open dataset.



Supplementary Fig. 7. Photograph of the experimental setups. The whole setup includes three parts: optical system, sample loader and electrical measurement system.

References

1. Liu, W. et al. Graphene charge-injection photodetectors. *Nature Electronics* 5, 281 (2022).
2. Goossens, S. et al. Broadband image sensor array based on graphene-CMOS integration. *Nature Photonics* 11, 366 (2017).